

## THE ENERGETIC STABILITY OF TORI AND SINGLE-WALL TUBES

Mircea V. Diudea<sup>1,\*</sup> and Edward C. Kirby<sup>2</sup>

<sup>1</sup>Faculty of Chemistry and Chemical Engineering,  
Babes-Bolyai University, 3400 Cluj, Romania

<sup>2</sup>Resource Use Institute, 14 Lower Oakfield, Pitlochry,  
Perthshire PH16 5DS, Scotland, UK

### ABSTRACT

Tessellated tori, generated here from square-like tiled lattices, are closely related to cylinders and capped tubes. This way of building them enables the orientation of their bonds, and so the geometric proportions of the torus, to be specified for molecular mechanics calculations and, along with their transformation into capped tubes this is illustrated and discussed in the light of their energetic stability.

### INTRODUCTION

Novel elemental forms of carbon besides ancient graphite and diamond, have been designed and synthesised by laser irradiation of graphite.<sup>1</sup> Finite molecular cage structures have been synthesised, characterised, functionalized or inserted into some supramolecular compounds.<sup>2–7</sup> However, the spherical surface cannot be tessellated by hexagons alone, so that other surfaces whose topology is

---

\* Corresponding author.

able to accommodate polyhexes and other energetically favoured patterns have also been investigated. Thus, besides the well known near-spherical fullerenes, cylinders, capped tubules and tori have aroused both theoretical and experimental interest.<sup>8–63</sup> Combinations of  $C_4$ , to  $C_8$  polygons, arranged in different ways, were proposed for pure carbon,<sup>64</sup> and work has also been done on multi elemental large cages.<sup>65–68</sup>

An important question about a toroidal network concerns its preferred shape. If the two pairs of opposite sides of a rectangular network are ‘identified’ or ‘glued’ together, to form first a tube and then a torus, the shape of the torus will depend on the order in which this is done. It can—as it were—be made by joining the ends of a long thin tube or a short fat one. These two extremes are topologically interchangeable and, furthermore, the tube may possibly deviate from having a circular cross section, so that the torus becomes more like a double walled cylinder. The particular shape adopted can of course be expected to depend on where the energy minimum with respect to bond distortions lies.

The Adjacency Matrix Eigenvectors Method (AME),<sup>63,64,69</sup> and the programmed algorithm NiceGraph, part of the Vega package published in Ljubljana<sup>70</sup> gives some qualitative information. The latter employs a spring-embedder routine to optimise the 3D drawing of a graph, and drawings of the thirteen hypothetical  $C_{60}$  toroidal benzenoids were shown in reference<sup>51</sup> and compared with the available rectangular polyhex precursors.

Borštnik and Lukman<sup>22</sup> were among the first to conduct Molecular Mechanics studies on toroidal polyhexes and toroidal polyhexes containing some  $C_5, C_7$  pairs, but this was to compare the tori with spherical fullerenes rather than to compare different shapes of a torus. Here we report a study, by Molecular Mechanics, of the energy of tori constructed so as to have particular bond orientations relative to the torus tube. We report also the generation of these in a novel way, by starting from a torus in whose surface is embedded a network of squares, and from which bonds are deleted on a systematic basis to form a polyhex system. The same technique allows tori with  $C_4, C_8$  and  $C_5, C_7$  patterns, and a number of the toroidal ‘twisted’ isomers, to be constructed.

## TOROIDAL NET GENERATION

Covering a toroidal surface by hexagons (and other polygons) in particular orientations is one of the main aims of this paper. The graphite zone-folding is the basic procedure in this respect. The method defines an equivalent planar parallelogram,<sup>37,54,61,71</sup> on the graphite sheet and identifies a pair of opposite sides to form a tube. Finally the two ends of the tube are glued in order to form a torus.

A number of notations have been used to define a toroidal polyhex. For example, Klein and others<sup>72</sup> used four parameters to describe a 'notched' rectangle used as the precursor; while John,<sup>54</sup> and Marušić & Pisanski<sup>71</sup> referred to a toroidal polyhex as  $\mathbf{T}_{p,q,t}$  where  $p$  and  $q$  count the hexagons stacked in a  $p \times q$  parallelogram and  $t$  counts the number of hexagons offset before final gluing. Kirby and his co-workers also used three parameters, in a similar but slightly different way, to define the torus where  $a$ ,  $b$ , and  $d$  define the biperiodic pattern of labelled hexagons that can be obtained by mapping the toroidal surface onto a planar honeycomb.<sup>20</sup> Here we base our general notation on the  $\mathbf{T}_{p,q,t}$  method mentioned above, with elaborations to be described, but in the case of toroidal polyhexes we also give the TPH  $a,b,d$  codes, because this method enables an exact canonical identification of the species involved to be made, and eigenvalues calculated.<sup>45</sup>

The present procedure starts from a square-like net embedded on a toroidal surface, generated according to an elementary geometry (see ref. 73). To generate a torus  $\mathbf{T}_{c,n}$  a cycle that initially is of indeterminate size is threaded with a  $c$ -membered cycle which is then copied to give  $n$  images of itself equally spaced around the other cycle. Every pair of images is connected by joining pairs of vertices resulting in a torus tiled with squares. We now proceed to remove certain edges in order to change the quadrilaterals into hexagons or other tiling patterns of chemical interest, and several cutting procedures have been developed.<sup>73</sup>

Thus, the square-like torus,  $\mathbf{T}_{c,n,C4}$  is completely defined by two integers:  $c$ -membering of the circulant polygon and  $n$ -membering of the large circle (i.e., the number of joined images of that polygon). The subscript C4 specifies the 4-membered cycle of the covering pattern. Note that the notation for this paper will be further elaborated, as necessary, to distinguish isomers. In case of single-wall tori, the square-like net consists of  $c \times n$  vertices,  $c \times n$  quadrilaterals and  $4 \times c \times n/2$  edges, 4 being the vertex degree of the net (which is a regular graph). The above relations come out as a consequence of Euler's formula:  $v - e + f = 2 - 2g$  ( $v$ ,  $e$ ,  $f$ ,  $g$  being respectively the number of vertices, number of edges, number of faces, and genus - unity, in case of a torus).

## CUTTING PROCEDURES

Standard C6 cutting: A cutting operation consists of deleting appropriate edges in a square-like lattice in order to produce hexagons or other combinations of polygonal faces.<sup>74</sup>

By deleting each second *horizontal* edge and alternating edges and cuts in each second row it results in a standard *h,C6 pattern* (Fig. 1 (a), top).

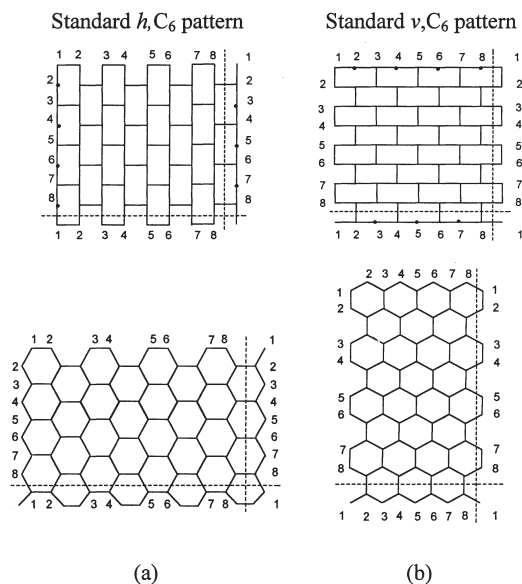


**Figure 1.** Standard C6-patterns and their optimised forms. Both the (a) and (b) forms here represent the same torus pattern, whose canonical code can be identified as  $TPH(8,0,4)^{45, 75}$  although the embeddings differ in their orientation with respect to the torus.

After optimising by a molecular mechanics program, an angular hexagonal pattern with respect to the larger diameter of the torus (referred to as a phenanthrenoid pattern) appears on the torus (Fig. 1 (a), bottom). A vertical action of the above algorithm leads to a standard  $v,C_6$  pattern (Fig. 1, (b)). It means that, after optimisation, a linear isomeric (anthracenoid) pattern is obtained (Fig. 1 (b), bottom).

From Fig. 1, it is obvious that each hexagon takes exactly two squares in the original square-like net. By construction, the number of hexagons in the  $h,C_6$  pattern is half the number of quadrilaterals on dimension  $c$  of the torus  $T_{c,n}$  while in the  $v,C_6$  pattern the reduced number of hexagons appears on dimension  $n$ . We stress here that the above cutting procedure *leaves unchanged the number of vertices in the original square-like torus*. The name of a polyhex torus thus generated, should reflect the type of cutting,  $h$  or  $v$ , as well as the tiling pattern.

Usually, tori have  $c < n$ , as follows from mathematical definition of the toroidal surface. As dimension  $c$  increases, exceeding the  $n$  dimension, the shape of toroidal net changes by assuming a more cylindrical form and finally reverts to the familiar 'doughnut' shape but with a thinner tube. Fig. 2 illustrates such  $h,C_6$ -tessellated tori. The molecular mechanics energy (in kcal/mol) increases

(i.e., it becomes less stable) for the tube generated (see Fig. 1.) from a higher  $h$ -value parallelogram.

Note that, especially in the case of thinner lattice precursors that form tubes of smaller radius, but also when a large-tubed torus adopts a double walled cylinder shape, the surface deviates from the ideal of being everywhere locally coplanar. This is because the prescribed length of atomic radii push the hexagons out of the plane of the cylindrical surface. In a  $v$ ,C6 pattern, the  $c$ -dimension is, by construction, twice as high as that shown by the  $h$ ,C6 pattern (That is, the number of hexagons on the  $c$ -dimension is double). Fig. 3 illustrates the corresponding pair, with an anthracenoid pattern.

As in case of the  $h$ ,C6 pattern, the thinner isomer shows a higher energy value than the corresponding larger isomer. For comparison, the torus  $T_{24,24,C6}$  is shown in both  $h$  and  $v$  cut forms in Fig. 4. It appears that the energy of the  $v$ ,C6 isomer is about double that shown by the  $h$ ,C6 isomer. The ratio of their heights is also close to two.

For these untwisted isomers, the relative molecular mechanics energy for the  $v$ -(i.e., anthracenoid) patterns is always the larger. In other words, these  $v$ -isomers are, so far without exception, predicted to be less stable than the corresponding  $h$ -isomers.

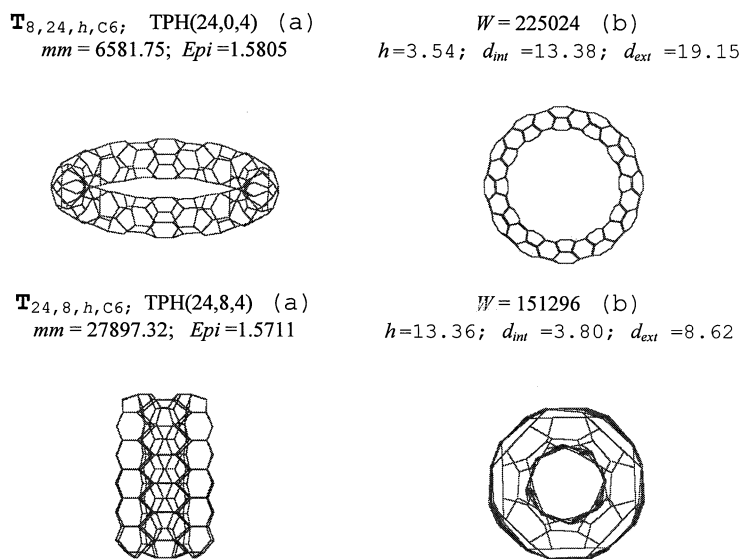
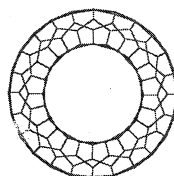
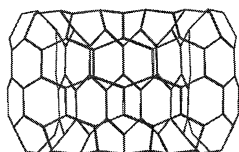


**Figure 2.** Polyhex tori  $h$ ,C6 patterned: (a) side view; (b) top view; TPH code, Wiener index  $W$ , relative molecular mechanics energy  $mm$  (kcal/mol); Huckel pi energy/atom  $E_{pi}$ , height  $h$ , interior and exterior diameters,  $d_{int}$  and  $d_{ext}$ , respectively (Angstroms).

$\mathbf{T}_{8,24,v,C6}$ ; TPH(24,8,4) (a)  
 $mm = 10415.08$ ;  $Epi = 1.5711$

$W = 151296$  (b)  
 $h = 7.46$ ;  $d_{int} = 6.95$ ;  $d_{ext} = 12.07$



$\mathbf{T}_{24,8,v,C6}$ ; TPH(24,0,4) (a)  
 $mm = 73678.56$ ;  $Epi = 1.5805$

$W = 225024$  (b)  
 $h = 25.45$ ;  $d_{int} = 2.10$ ;  $d_{ext} = 6.21$

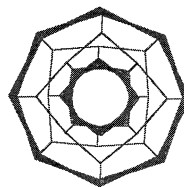
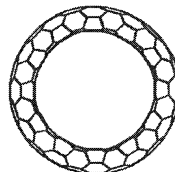
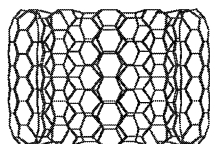


**Figure 3.** Polyhex tori  $v,C6$  patterned: (a) side view; (b) top view.

$\mathbf{T}_{24,24,h,C6}$ ; TPH(24,0,12) (a)  
 $mm = 14713.75$ ;  $Epi = 1.5740$

$W = 2320128$  (b)  
 $h = 13.16$ ;  $d_{int} = 13.85$ ;  $d_{ext} = 19.53$



$\mathbf{T}_{24,24,v,C6}$ ; TPH(24,0,12) (a)  
 $mm = 31686.80$ ;  $Epi = 1.5740$

$W = 2320128$  (b)  
 $h = 24.08$ ;  $d_{int} = 6.86$ ;  $d_{ext} = 12.12$

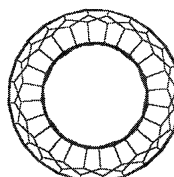
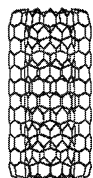


**Figure 4.** Polyhex tori  $h,C6$  and  $v,C6$  patterned: (a) side view; (b) top view.

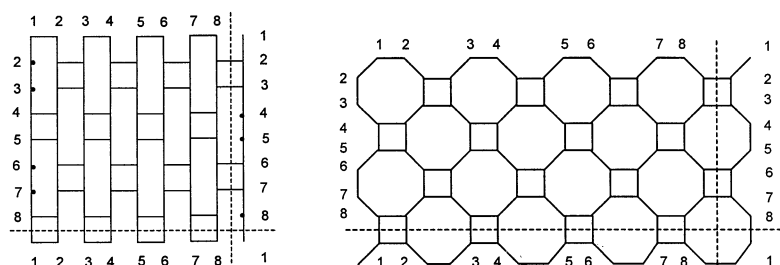


Figure 5. An  $h,C_4,C_8$ -pattern and its optimised form.

### OTHER PATTERN CONSTRUCTIONS

As already mentioned, in tessellating a toroidal surface, some other patterns beside polyhex ones have also been considered.<sup>74, 76</sup> An alternating  $C_4,C_8$  pattern was depicted in reference<sup>28</sup> (see also reference 77). In our procedure, this pattern results by following the principle of alternating edges and cuts and keeping the same any two subsequent rows or columns. The cutting illustrated in Fig. 5 is performed horizontally. This pattern has been used for tiling spherical fullerenes.<sup>78</sup>

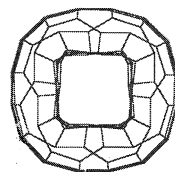
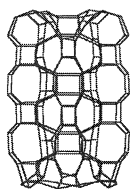
The tori corresponding to this are illustrated in Fig. 6. Note that, the  $h,C_4,C_8$ -pattern is identical to the  $v,C_4,C_8$ -pattern. However, the isomeric tori will be

$$\mathbf{T}_{24,8,h,C_4,C_8} \quad (\text{a})$$

$$mm = 20993.53; \quad Epi = 1.4680$$

$$W = 155136 \quad (\text{b})$$

$$h = 13.33; \quad d_{int} = 3.97; \quad d_{ext} = 11.72$$



$$\mathbf{T}_{24,8,v,C_4,C_8} \quad (\text{a})$$

$$mm = 68700.16; \quad Epi = 1.4810$$

$$W = 240384 \quad (\text{b})$$

$$h = 32.29; \quad d_{int} = 2.51; \quad d_{ext} = 5.38$$

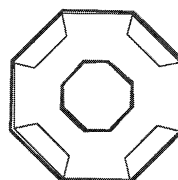
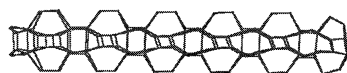


Figure 6.  $C_4,C_8$  isomers of  $T_{24,8}$ : (a) side view; (b) top view.

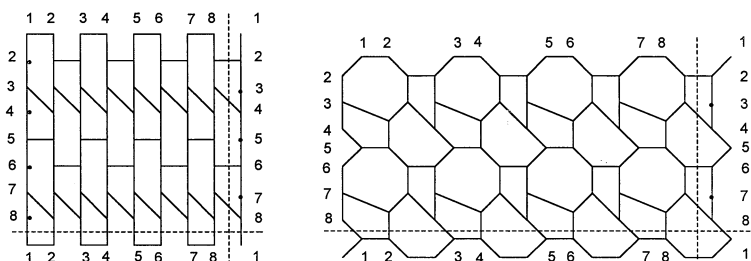


Figure 7. An  $h,C_5,C_7$ -pattern.

different, as a consequence of anisotropy of the cutting algorithm. Observe the shifting of corresponding dimensions. Pentagons and heptagons can reduce strain when they are introduced at suitable positions within a tubular polyhex net.<sup>22, 63</sup> When a pure  $C_5,C_7$  pattern is used, the lattice is called azulenoïd.<sup>28</sup> or pentaheptite.<sup>79</sup>

The pentalene (i.e., two fused five-membered rings) apparition is not a steric backtracking in tori - since a more pronounced curvature occurs here - in contrast to the spherical fullerenes.

In the present procedure, the construction of a pure  $C_5,C_7$ -cutting needs four rows (columns) of square-like faces (i.e., a  $(0 \bmod 4)$  lattice - Fig. 7). In the case of a  $(2 \bmod 4)$  net, or incomplete use of the  $C_6$  net, it results in a  $C_5,C_6,C_7$ -pattern (Fig. 8).

Fig. 9 illustrates the isomers of  $T_{24,8}$  covered by the  $C_5,C_7$ -pattern. Observe that introducing various dissimilar polygons in the tube-shaped lattice, forces it to adopt some degree of twisting. The twisting is higher for the  $C_5,C_7$  pattern and correspondingly for the  $\nu$ -net. Correspondingly, a drop in energy values is observed: from 27897.32 kcal/mol for  $T_{24,8,h,C_6}$  to 23001.46, in case of  $T_{24,8,h,C_5,C_7}$  and from 73678.56 kcal/mol for  $T_{24,8,\nu,C_6}$  to 54964.83, in case of  $T_{24,8,\nu,C_5,C_7}$ .

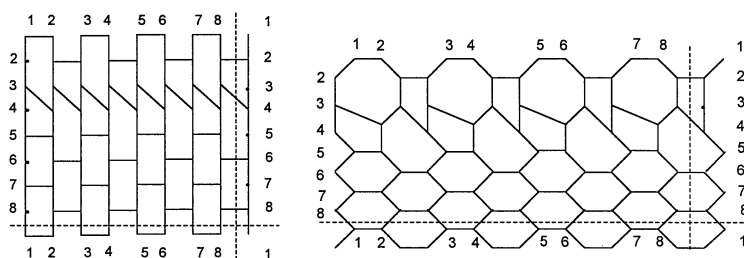
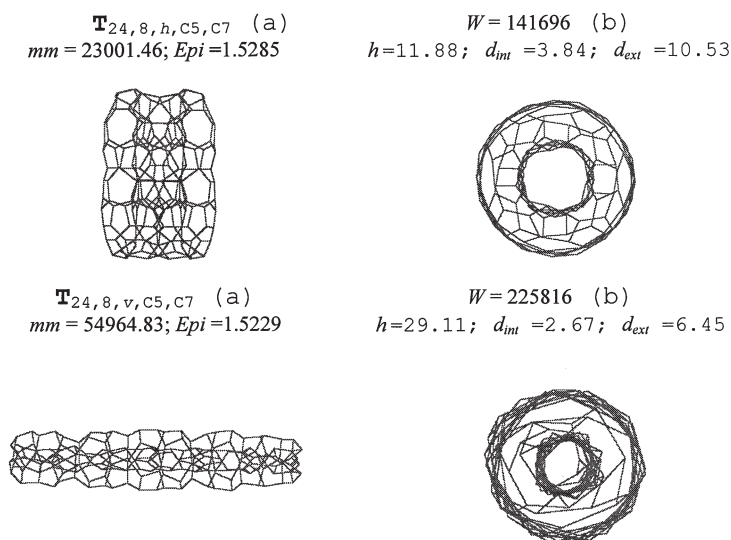


Figure 8. An  $h,C_5,C_6,C_7$ -pattern.

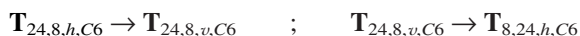




**Figure 9.**  $C_5, C_7$  isomers of  $T_{12,24}$ : (a) side view; (b) top view.

A note of caution must be entered here, since by enlarging the torus, besides a drop in energy value per atom (145.3 kcal/atom for  $\mathbf{T}_{24,8,h,C6}$  to 25.5 for  $\mathbf{T}_{24,24,h,C6}$  and from 383.74 kcal/atom in  $\mathbf{T}_{24,8,v,C6}$  to 55.01 in  $\mathbf{T}_{24,24,v,C6}$ ), a different trend could appear.

Concerning lattice stability, within MM optimisation, the relatively unstable structures rearrange to more stable ones. Two examples are given in this respect:



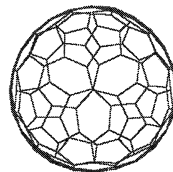
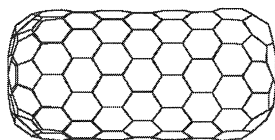
The relatively stable structures, such as  $\mathbf{T}_{8,24,h,C6}$  or  $\mathbf{T}_{8,24,v,C6}$ , keep their own net.

### CAPPED TUBES FORMED BY OPENING TORI

By cutting some edges within a torus, a spanning tube is obtained. The cutting may operate on either horizontal or vertical edges. Attention is focussed on cutting more tube-like tori in this way, without an exhaustive enumeration of all possible isomers (that can arise from both the type of cutting and the type of capping). In the following, we illustrate some classes of single-wall, capped tubes, originating in the tori already discussed.

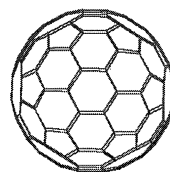
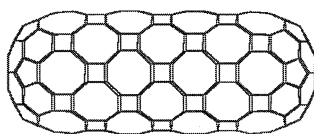
**TU**<sub>24,8,h,C6,v</sub> (a)  
 $mm = 1045.03$   
 $Epi = 1.5681$

$W = 267038$  (a)  
 $h = 17.86$ ;  $d = 9.37$   
 236 atoms; added 44 to **T**<sub>24,8,h,C6</sub>



**TU**<sub>24,8,h,C4,C8,v</sub> (a)  
 $mm = 4937.13$   
 $Epi = 1.4773$

$W = 297624$  (b)  
 $h = 21.75$ ;  $d = 9.21$   
 240 atoms; added 48 to **T**<sub>24,8,h,C8</sub>



**TU**<sub>24,8,h,C5,C7,v</sub> (a)  
 $mm = 1242.69$   
 $Epi = 1.5199$

$W = 302419$  (b)  
 $h = 22.97$ ;  $d = 8.96$   
 248 atoms; added 56 to **T**<sub>24,8,h,C5,C7</sub>

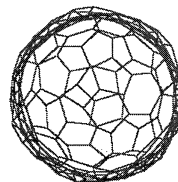
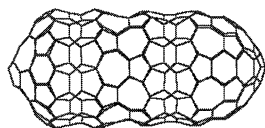


**Figure 10.** Capped tubes obtained by vertical cutting of an *h*-net.

First (Fig. 10) a class is obtained by vertical cutting of a net (particularly an *h*,C6 net). The next three examples are relatively short tubes, showing a level of energy lower than for the corresponding tori by 1–2 orders of magnitude. The minimum value is shown by **TU**<sub>24,8,h,C6,v</sub> (4.4 kcal/atom).

The  $h$ ,C6 net can be cut horizontally, resulting in a second class of tubes. The examples given in Fig. 11 show a level of energy ranging from 8.5 for  $\text{TU}_{24,8,h,\text{C6},h}$  to 5.5 for  $\text{TU}_{24,8,h,\text{C5},\text{C7},h}$ . Observe the last superscript  $v$  or  $h$ , indicating the type of cutting of the original torus.

A third class of tubes considered here represent the thinnest possible tubes, with no triangles. As discussed above, the phenanthrenoid lattice differs from the

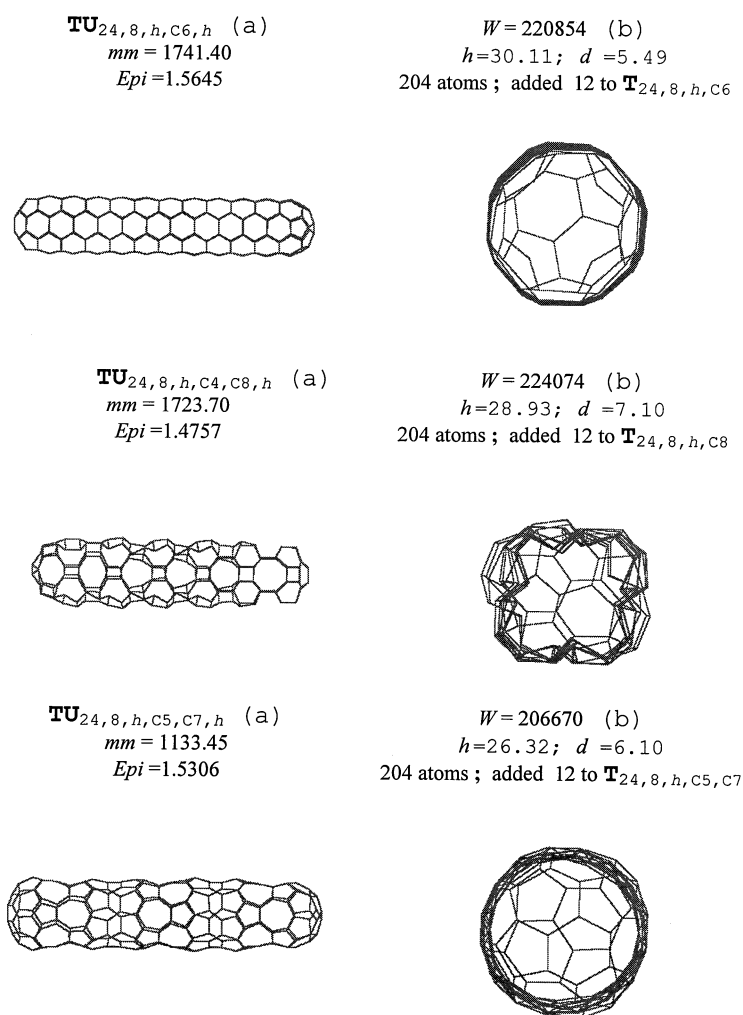
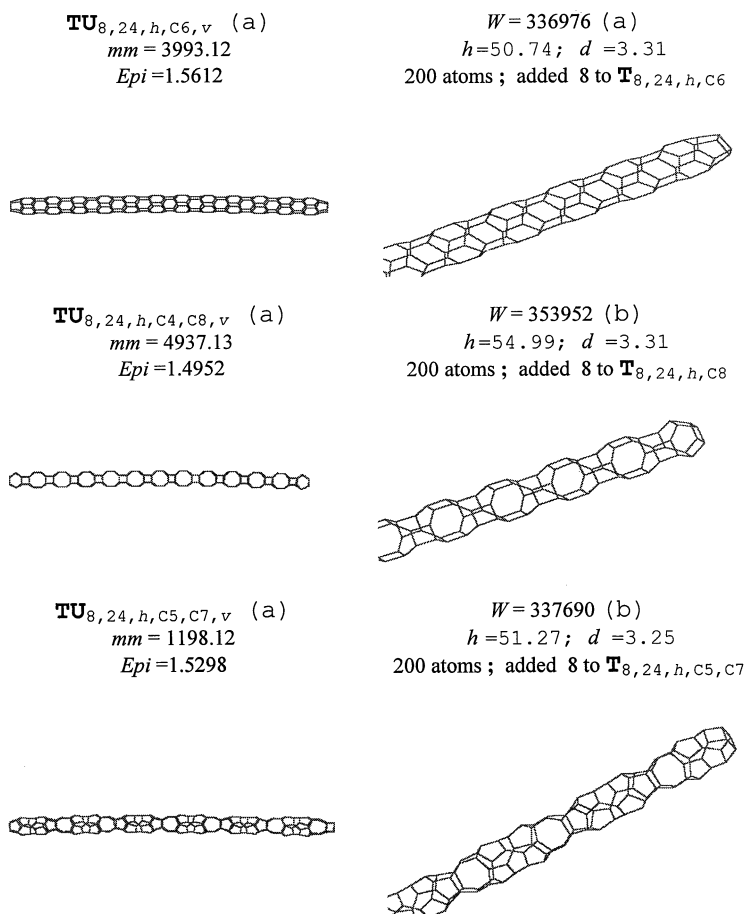


Figure 11. Capped tubes obtained by horizontal cutting of an  $h$ -net.



**Figure 12.** The thinnest possible capped tubes without triangles, obtained by vertical cutting of an  $h,C_6$  net.

anthracenoid one both by the shape of capping and energy. Only the vertical cutting is discussed in the following.

In case of an  $h,C_6$  net, the resulting tube is an anthracenoid with respect to its ends. The mixed  $h,C_5,C_7$  net (with 5.99 kcal/atom in  $\text{TU}_{8,24,h,C5,C7,v}$ ) appears to be the most stable one among the  $h,C_6$  net originating class.

The tubes obtained from a  $v,C_6$  net (Fig. 13) are phenanthrenoid isomers with the highest stability (i.e., lower energy) shown again by a  $C_5,C_7$  net (10.16 kcal/atom in  $\text{TU}_{4,48,v,C5C7,v}$ ). Their energy values are higher in comparison to those shown by the corresponding anthracenoid isomers (see above).

## TWISTED TORI

Let now consider a twisted square-like lattice (Fig. 14) and follow the same principle of cutting. Different patterns appear, as a function of the number of row faces affected by twisting. In case of an odd number of twisted rows (denoted here by  $t_1$ ), two rows of alternating C4, C8 polygons appear among the C6 ones. Alternatively, when the number of rows is even (marked by  $t_2$ ), a pure  $h$ C<sub>6</sub> pattern results, as has been extensively discussed in earlier work.<sup>19,20,45,72</sup>

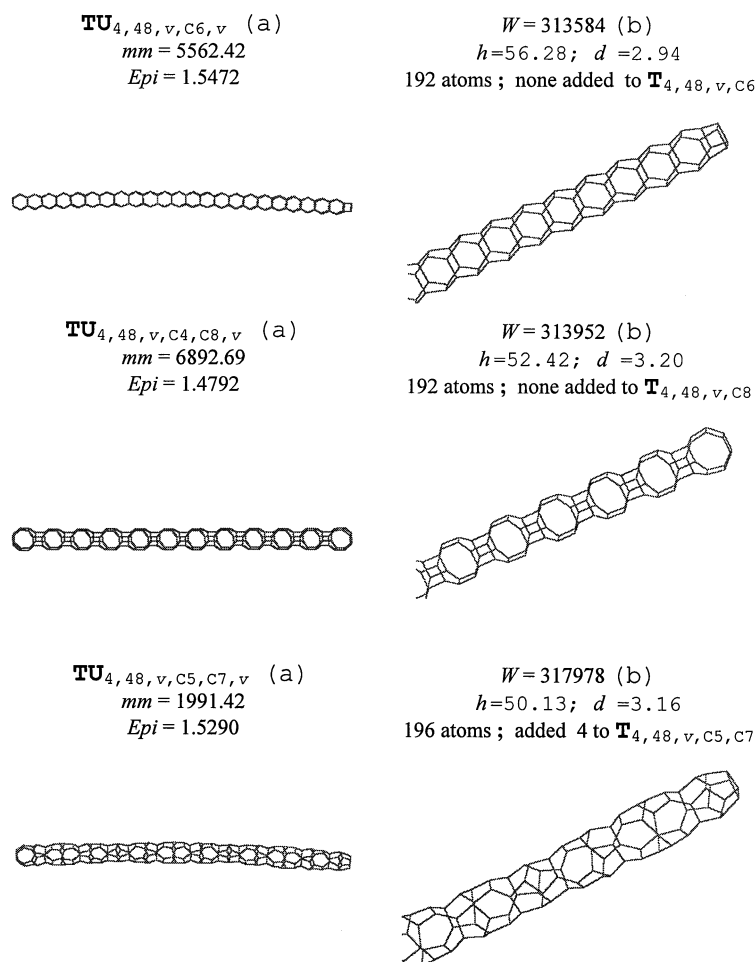
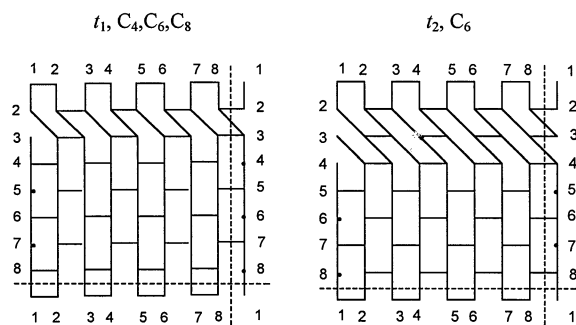
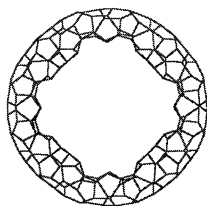


Figure 13. Smallest possible capped tubes obtained by vertical cutting of a  $v$ C<sub>6</sub> net.

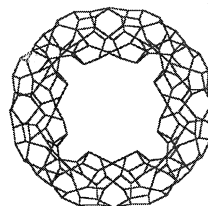


**Figure 14.** The patterns obtained as a result of applying the cutting procedure to a square-like lattice when this extends over, respectively, an odd and an even number of rows of faces.

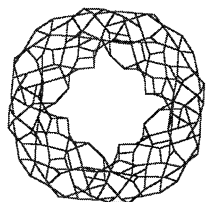
$\mathbf{T}_{8,24,t2,h,C6}$   
 $mm = 13831.32; Epi = 1.5790$   
 $TPH\ 96,39,1 = 32,5,3$   
 $W = 199872$



$\mathbf{T}_{8,24,t4,h,C6}$   
 $mm = 31755.52; Epi = 1.5756$   
 $TPH\ 48,6,2 = 16,2,6$   
 $W = 174336$



$\mathbf{T}_{8,24,t6,h,C6}$   
 $mm = 57682.55; Epi = 1.5751$   
 $TPH\ 97,7,1 = 16,7,6$   
 $W = 152832$



$\mathbf{T}_{8,24,t8,h,C6}$   
 $mm = 85459.35; Epi = 1.5749$   
 $TPH\ 24,12,4 = 8,0,12$   
 $W = 142272$

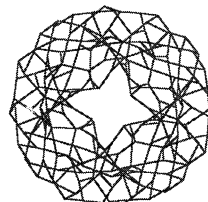


**Figure 15.** The optimised form of some twisted  $h,C6$  pattern tori.

In the following, we consider only  $h, C_6$  patterns. The optimised form of some twisted tori are illustrated in Fig. 15.

A different twisting is induced by rhomboidal lattices, as shown in Fig. 16: in case (a) the pattern  $rh, l$  is built up by de novo generation of a rhombic pattern while the pattern  $rh, h$ , case (b) is derived from a square-like net. It is expected that in case (a) the twisting is  $\pi/4$  while in case (b) the angle could be different, due to some distortions of the net. This kind of twisting is equivalent to some off set in the final gluing of a long tube to give a torus. Our goal is to obtain tubes by cutting tori and such a procedure will provide untwisted tubes starting from rhomboidal lattices.

Conversely, the twisting induced by twisted square-like lattices is intrinsic and the twisting remains in the corresponding tubes. (Fig. 18).

### CONCLUSIONS

The results confirm that untwisted thin-tubed tori are predicted to be more stable. Thus, from structure  $T_{8,24,h,C6}$  to  $T_{8,24,v,C6}$  and within the sequence

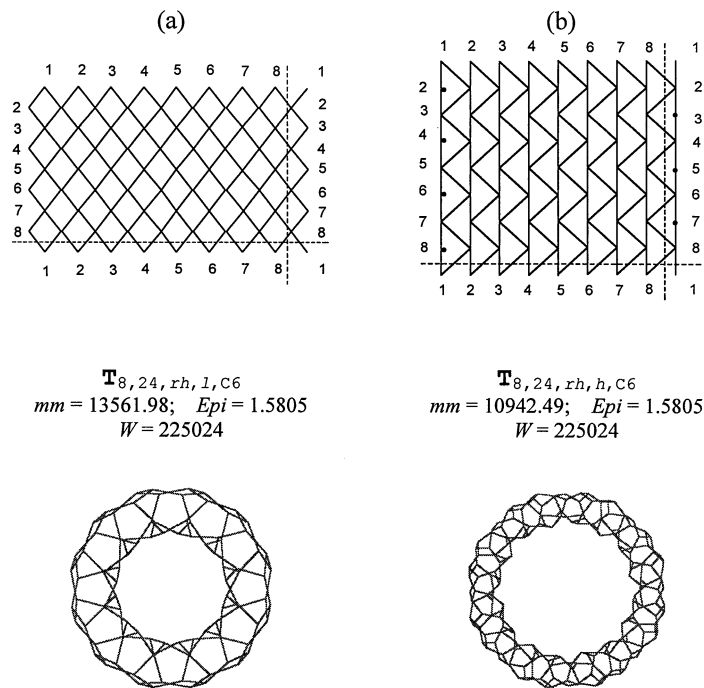


**Figure 16.** Rhomboidal patterns:  $rh, l$  (a) and  $rh, h$  (b) and corresponding optimised toroidal structures.

$$\begin{aligned} &\mathbf{TU}_{8,24,rh,l,C6,v} \\ &mm = 4106.17; \quad Epi = 1.5681 \\ &W = 336976; \quad 200 \text{ atoms} \end{aligned}$$

$$\begin{aligned} &\mathbf{TU}_{8,24,rh,h,C6,v} \\ &mm = 4106.33; \quad Epi = 1.5681 \\ &W = 336976; \quad 200 \text{ atoms} \end{aligned}$$

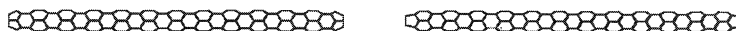


**Figure 17.** The rhomboidal patterned tori of Fig. 16 provide untwisted tubes.

$$\begin{aligned} &\mathbf{TU}_{8,24,t2,h,C6,v} \\ &mm = 3664.71; \quad Epi = 1.5687 \\ &W = 299731; \quad 202 \text{ atoms} \end{aligned}$$

$$\begin{aligned} &\mathbf{TU}_{8,24,t4,h,C6,v} \\ &mm = 2798.45; \quad Epi = 1.5639 \\ &W = 296412; \quad 212 \text{ atoms} \end{aligned}$$



$$\begin{aligned} &\mathbf{TU}_{8,24,t6,h,C6,v} \\ &mm = 1993.24; \quad Epi = 1.5656 \\ &W = 263342; \quad 214 \text{ atoms} \end{aligned}$$

$$\begin{aligned} &\mathbf{TU}_{8,24,t8,h,C6,v} \\ &mm = 1483.28; \quad Epi = 1.5666 \\ &W = 252450; \quad 220 \text{ atoms} \end{aligned}$$



**Figure 18.** Twisted capped tubes spanned from twisted  $h,C6$  lattices of Fig. 15.

$T_{8,24,ix,h,C6}$ , ( $x = 2, 4, 6, 8$ ) there is an increase in MM energy. Furthermore, this trend can be roughly predicted by how nearly equal are the two dimensions of the most compact parallelogram<sup>51</sup> from which the toroidal lattice can be constructed.

Notice the equivalences:  $T_{24,8,h,C6} = T_{8,24,v,C6}$ ;  $T_{24,8,v,C6} = T_{8,24,h,C6}$ , and  $T_{8,24,rh,l,C6} = T_{8,24,rh,h,C6}$  which are entirely natural (each pair refers to two embeddings of the same closed lattice on the torus).



## REFERENCES

1. H. Kroto, *The First Predictions in the Buckminsterfullerene Crystal Ball*. Fullerene Sci. Technol., 1994, 2, 333–342.
2. F. Diedrich and C. Thilgen, *Covalent Fullerene Chemistry*. Science, 1996, 271, 317–323.
3. H. Zorc, Lj. P. Toli, S. Martinovi, and D. Srzi, *Synthesis and Laser Desorption: Fourier Transform Mass Spectrometry of Massive Fullerenes*. Fullerene Sci. Technol., 1994, 2, 471–480.
4. I. S. Neretin, K. A. Lyssenko, M. Yu. Antipin, Yu. L. Slovokhotov, O. V. Boltalina, P. A. Troshin, A. Yu. Lukonin, L. N. Sidorov, and R. Taylor, *C<sub>60</sub>F<sub>18</sub>, a Flattened Fullerene: Alias a Hexa-Substituted Benzene*. Angew. Chem. Int. Ed., 2000, 39, 3273–3276.
5. W. Rubin Qian, Y., *A Parallel Library of All Seven A<sub>2</sub> + B<sub>2</sub> + C<sub>2</sub> The Regioisomeric Hexakisadducts of Fullerene C<sub>60</sub>: Inspiration from Werner's Octahedral Stereoisomerism*. Angew. Chem. Int. Ed., 2000, 39, 3133–3137.
6. K. Lee, Ch. Lee, H. Song, J. T. Park, H. Y. Chang, and M.-G. Choi, *Interconversion between  $\mu - \eta^2, \eta^2 - C_{60}$  and  $\mu_3 - \eta^2, \eta^2 - C_{60}$  on a Carbido Pentaosmium Cluster Framework*. Angew. Chem. Int. Ed., 2000, 39, 1801–1804.
7. T.F. Fässler, R. Hoffmann, S. Hoffmann, and M. Wörle, *Triple-Decker Type Coordination of Fullerene Trianion in [K([18] crown-6)]<sub>3</sub>-[ $\eta^6, \eta^6 - C_{60}$ ]( $\eta^3 - C_6H_5CH_3$ )<sub>2</sub> - Single Crystal Structure and Magnetic Properties*. Angew. Chem. Int. Ed., 2000, 39, 2091–2094.
8. T.G. Schmalz, W.A. Seitz, D.J. Klein, and G.E. Hite, *Elemental Carbon Cages*. J. Am. Chem. Soc., 1988, 110, 1113–1127.
9. C. Thomassen, *Tilings of the Torus and the Klein Bottle and Vertex-transitive Graphs on a Fixed Surface*. Trans. Am. Math. Soc., 1991, 323, 605–635.
10. S. Iijima, *Helical Microtubules of Graphitic Carbon*. Nature, 1991, 354, 56–58.
11. R. Tosić and S.J. Cyvin, *Hypothetical Structure for the C<sub>60</sub> Cluster: A toroid*. Zb. Radova Prirod.-Matemat. Fak. Univ. Novom Sadu, 1992, 22.
12. H. Hosoya and Y. Tsukano, *2-Dimensional Torus Benzenoids whose Electronic State Rapidly Converges to Graphite*. Conference paper at ISNA-7, International Symposium on Novel Aromatic Compounds, Victoria B.C., Canada, 1992.
13. S. Itoh and S. Ihara, *Toroidal Forms of Graphite Carbon II. Elongated Tori*. Phys. Rev. B, 1993, 48, 8323–8328.
14. S. Itoh and S. Ihara, *Toroidal Form of C<sub>360</sub>*. Phys. Rev. B, 1993, 47, 1703–1704.
15. S. Ihara and S. Itoh, *Toroidal Forms of Graphitic Carbon*. Phys. Rev. B, 1993, 47, 12908–12911.

16. P. E. John and B. Walther, *Mögliche Strukturen und Linearfaktoranzahlen toroidaler hexagonaler Systeme*. 1993, Techn. Univ. Ilmenau, Fak. Math. Naturwiss.
17. H. Hosoya, Y. Tsukano, M. Ohuchi, and K. Nakada. *Two-Dimensional Torus Benzenoids whose Electronic State Rapidly Converges to Graphite*. Conference paper given at International Conference & Exhibition. *Computer Aided Innovation of New Materials*, 1993, Fac. Sci., Ochanomizu Univ., Tokyo, Japan, 112.
18. S. Iijima and T. Ichihashi, *Single-Shell Carbon Nanotubes of 1 nm Diameter*. *Nature*, 1993, *361*, 603–605.
19. E. C. Kirby, *Cylindrical and Toroidal Polyhex Structures*. *Croat. Chem. Acta*, 1993, *66*, 13–26.
20. E. C. Kirby, R. B. Mallion, and P. Pollak, *Toroidal Polyhexes*. *J. Chem. Soc. Faraday Trans.*, 1993, *89*, 1945–1953.
21. M. Randić, Y. Tsukano, and H. Hosoya, *On Enumeration of Kekulé Structures for Benzenoid Tori*. *Natural Sci. Rep. Ochanomizu Univ.*, 1994, *45*, 101–119.
22. B. Borštnik and D. Lukman, *Molecular Mechanics of Toroidal Carbon Molecules*. *Chem. Phys. Letters*, 1994, *228*, 312–316.
23. S. Itoh and S. Ihara, *Isomers of the Toroidal Forms of Graphite Carbon*. *Phys. Rev. B – Condens. Matter*, 1994, *49*, 13970–13974.
24. P. E. John and B. Walther, *Sketch about Possible Structures and Numbers of Perfect Matchings of Toroidal Hexagonal Systems*. 1994, Techn. Univ. Ilmenau, Fak. Math. Naturwiss.
25. J.K. Johnson, B.N. Davidson, M.R. Pederson, and J.Q. Broughton, *Energetics and Structure of Toroidal Forms of Carbon*. *Phys. Rev. B – Condens. Matter*, 1994, *50*, 17575–17582.
26. J.C. Greer, S. Itoh, and S. Ihara, *Ab Initio Geometry and Stability of a C<sub>120</sub> Torus*. *Chem. Phys. Lett.*, 1994, *222*, 621–625.
27. H. Sachs, *Graph Theoretical Means for Calculating Kekulé and Huckel Parameters in Benzenoid and Related Systems*. *J. Chem. Inf. Comput. Sci.*, 1994, *34*, 432–435.
28. E. C. Kirby, *On Toroidal Azulenoids and Other Shapes of Fullerene Cage*. *Fullerene Sci. Technol.*, 1994, *2*, 395–404.
29. E. C. Kirby, *Remarks upon Recognising Genus and Possible Shapes of Chemical Cages in the Form of Polyhedra, Tori and Klein Bottles*. *Croat. Chem. Acta*, 1995, *68*, 269–282.
30. J. E. Avron and J. Berger, *Tiling Rules for Toroidal Molecules*. *Phys. Rev. A*, 1995, *51*, 1146–1149.
31. M. Kaufman, T. Pisanski, D. Lukman, B. Borštnik, and A. Graovac, *Graph-drawing Algorithms Geometries Versus Molecular Mechanics in Fullerenes*. *Chem. Phys. Lett.*, 1996, *259*, 420–424.

32. J. Berger and J. E. Avron, *Classification Scheme for Toroidal Molecules*. J. Chem. Soc. - Faraday Trans., 1995, 91, 4037–4045.
33. A. Ceulemans and P. W. Fowler, *Symmetry Extensions of Euler's Theorem for Polyhedral, Toroidal and Benzenoid Molecules*. J. Chem. Soc. - Faraday Trans., 1995, 91, 3089–3093.
34. S. Ihara and S. Itoh, *Helically Coiled and Toroidal Cage Forms of Graphitic Carbon*. Carbon, 1995, 33, 931–939.
35. A. Sarkar, H.W. Kroto, and M. Endo, *Hemi-Toroidal Networks in Pyrolytic Carbon Nanotubes*. Carbon, 1995, 33, 51–55.
36. S. Ihara and S. Itoh, *Molecular Dynamics Study of Toroidal and Helically Coiled Forms of Graphitic Carbon*. Surface Rev. Lett., 1996, 3, 827–834.
37. E. C. Kirby, *Recent Work on Toroidal and Other Exotic Fullerene Structures*, in *From Chemical Topology to Three - Dimensional Geometry*, A. T. Balaban, Editor. 1997, Plenum Press: New York. p. 263–296.
38. D. J. Klein and H.Y. Zhu, *All-Conjugated Carbon Species*, in *From Chemical Topology to Three - Dimensional Geometry*, A. T. Balaban, Editor. 1997, Plenum Press: New York. p. 297–341.
39. K. Esfarjani, Y. Hashi, S. Itoh, S. Ihara, and Y. Kawazoe, *Stability and Vibrational Spectra of Toroidal Isomers of C-240*. Zeitsch. Physik D – Atoms, Molec. Clusters, 1997, 41, 73–76.
40. R. Setton and N. Setton, *Carbon Nanotubes .3. Toroidal Structures and Limits of a Model for the Construction of Helical and S-shaped Nanotubes*. Carbon, 1997, 35, 497–505.
41. R. C. Haddon, *Electronic Properties of Carbon Toroids*. Nature, 1997, 388, 31–32.
42. M. Yoshida, M. Fujita, P. W. Fowler, and E. C. Kirby, *Non-bonding Orbitals in Graphite, Carbon Tubules, Toroids and Fullerenes*. J.Chem. Soc. - Faraday Trans., 1997, 93, 1037–1043.
43. J. Liu, H. Dai, J. H. Hafner, D. T. Colbert, R. E. Smalley, S. J. Tans, and C. Dekker, *Fullerene 'Crop Circles'*. Nature, 1997, 385, 780–781.
44. C. G. Cash, *Simple Means of Computing the Kekulé Structure Count for Toroidal Polyhex Fullerenes*. J. Chem. Inf. Comput. Sci., 1998, 38, 58–61.
45. E. C. Kirby and P. Pollak, *How to Enumerate the Connectional Isomers of a Toroidal Polyhex Fullerene*. J. Chem. Inf. Comput. Sci., 1998, 38, 66–70 and 1256.
46. M. F. Lin and D. S. Chuu, *Electronic States of Toroidal Carbon Nanotubes*. J. Phys. Soc. Japan, 1998, 67, 259–263.
47. J.E. Avron and J. Berger, *Toroidal Graphitic Molecules*. Fullerene Sci. Technol., 1998, 6, 31–37.
48. M. F. Lin and D. S. Chuu, *Persistent Currents in Toroidal Carbon Nanotubes*. Phys. Rev. B, Condens. Matter, 1998, 57, 6731–6737.

49. M. F. Lin, *Magnetic Properties of Toroidal Carbon Nanotubes*. J. Phys. Soc. Japan, 1998, 67, 1094–1097.
50. V. Meunier, P. Lambin, and A. A. Lucas, *Atomic and Electronic Structures of Large and Small Carbon Tori*. Phys. Rev. B, Condens. Matter, 1998, 57, 14886–14890.
51. E. C. Kirby and T. Pisanski, *Aspects of Topology, Genus and Isomerism in Closed 3-valent Networks*. J. Math. Chem., 1998, 23, 151–167.
52. M. F. Lin, R. B. Chen, and F. L. Shyu, *Electronic Structures of Chiral Carbon Toroids*. Solid State Commun., 1998, 107, 227–231.
53. M. F. Lin, *Magneto-optical Properties of Carbon Toroids*. J. Phys. Soc. Japan, 1998, 67, 2218–2221.
54. P. E. John, *Kekulé Count in Toroidal Hexagonal Carbon Cages*. Croat. Chem. Acta, 1998, 71, 435–447.
55. G. G. Cash, *Double-Toroid, Almost-polyhex Fullerenes*. Fullerene Sci. Technol., 1999, 7, 147–158.
56. M. F. Lin, *Thermal Properties of Carbon Toroids*. J. Phys. Soc. Japan, 1999, 68, 3585–3591.
57. M. F. Lin, *Plasmons in Narrow-gap Carbon Toroids*. J. Phys. Soc. Japan, 1999, 68, 1102–1105.
58. M. F. Lin, *Magnetic Properties of Chiral Carbon Toroids*. Physica B, 1999, 269, 43–48.
59. M. F. Lin, *Electronic Collective Excitations in Thin Toroids*. Chinese J. Phys., 1999, 37, 498–508.
60. M. F. Lin, *Transport Properties of Carbon Toroids*. J. Phys. Soc. Japan, 1999, 68, 3744–3745.
61. A. Ceulemans, L. F. Chibotaru, S. A. Bovin, and P. W. Fowler, *The Electronic Structure of Polyhex Carbon Tori*. J. Chem. Phys., 2000, 112, 4271–4278.
62. P. W. Fowler, P. E. John, and H. Sachs, *(3,6)-Cages, Hexagonal Toroidal Cages, and Their Spectra*. DIMACS Series in Discr. Math. Theor. Comput. Sci., 2000, 51, 139–174.
63. A. Graovac, D. Plavšić, M. Kaufman, T. Pisanski, and E. C. Kirby, *Application of the Adjacency Matrix Eigenvectors Method to Geometry Determination of Toroidal Carbon Molecules*. J. Chem. Phys., 2000, 113, 1925–1931.
64. D. E. Manolopoulos and P. W. Fowler, *Molecular Graphs, Point Groups, and Fullerenes*. J. Chem. Phys., 1992, 96, 7603–7614.
65. A. Müller, P. Kögerler, and Ch. Kuhlmann, *A Variety of Combinatorially Linkable Units as Disposition: from a Giant Icosahedral Keplerate to Multi-Functional Metal-Oxide Based Network Structures*. Chem. Commun., 1999, 1347–1358.
66. R. B. King, *Novel Concepts in Carbon Allotrope Structures*. Concepts in Chemistry: A Contemporary Challenge, pp 133–151, ed. D.H. Rouvray. 1997, Taunton, England: Research Studies Press Ltd.

67. R. B. King, *Aromaticity from Planar Organic Molecules to Polyhedral Inorganic Species*. Concepts in Chemistry: A Contemporary Challenge, pp 153–199, ed. D.H. Rouvray. 1997, Taunton, England: Research Studies Press Ltd.
68. R. B. King, *Applications of Topology and Graph Theory in Understanding Inorganic Molecules*. From Chemical Topology to Three - Dimensional Geometry, pp 343–414, ed. A.T. Balaban. 1997, New York: Plenum Press.
69. P.W. Fowler, T. Pisanski, and J. Shawe-Taylor, eds. *Molecular Graph Eigenvectors for Molecular Coordinates*. Graph Drawing: Lecture Notes in Computer Science 894, ed. R. Tamassia and I.G. Tollis. 1995, Springer-Verlag.
70. T. Pisanski, *Vega Quick Reference Manual and Vega Graph Gallery*. 1995, Ljubljana. (Also at <http://vega:ijp.si/>.)
71. D. Marušić and T. Pisanski, *Symmetries of Hexagonal Molecular Graphs on the Torus*. Croat. Chem. Acta, 2000, 73, 969–981.
72. D. J. Klein, *Elemental Benzenoids*. J. Chem. Inf. Comput. Sci., 1994, 34, 453–459.
73. M. V. Diudea, A. Graovac and A. Kerber, *Generation and Graph-Theoretical Properties of C<sub>4</sub>-Tori*. MATCH, to appear.
74. M. V. Diudea, Silaghi-Dumitrescu, and B. Parv, *Toranes Versus Torenes*. MATCH, to appear.
75. Note: A toroidal polyhex can be defined by three numbers,  $a, b, d$ . The closed toroidal network is mapped onto an infinite planar tiling with hexagons, giving a biperiodic pattern. If one of the hexagons is labelled, then the positions where it repeats will enable one or more polyhex parallelograms to be outlined which represent the whole set of hexagons on the torus. From one of these markers, count hexagons until the label repeats itself at the  $a^{\text{th}}$  hexagon; return to the origin and count along the same row until, at the  $b^{\text{th}}$  hexagon, there is a repeat marker at 120 degrees to the forward direction; count up this diagonal until this last marker is found at the  $d^{\text{th}}$  hexagon. In general there are up to six possible  $a, b, d$ , triplets. The convention for choosing a canonical code is to choose one with minimum  $d$ , and from these, the one with minimum  $b$ .
76. M. V. Diudea and P. John, *Covering Polyhedral Tori*. MATCH, to appear.
77. T. Pisanski, A. Žitnik, A. Graovac, and A. Baumgartner, *Rotagraphs and their Generalizations*. J. Chem. Inf. Comput. Sci., 1994, 34, 1090–1093.
78. Y. D. Gao and W. C. Herndon, *Fullerenes with Four-Membered Rings*. J. Amer. Chem. Soc., 1993, 115, 8459–8460.
79. M. Deza, P. W. Fowler, M. Shtogrin, and K. Vietze, *Pentaheptite Modifications of the Graphite Sheet*. J. Chem. Inf. Comput. Sci., 2000, 40, 1325–1332.

Received: April 26, 2001





Copyright of Fullerene Science & Technology is the property of Marcel Dekker Inc. and its content may not be copied or emailed to multiple sites or posted to a listserv without the copyright holder's express written permission. However, users may print, download, or email articles for individual use.